The 30 May 1998 Spencer, South Dakota, Storm. Part II: Comparison of Observed Damage and Radar-Derived Winds in the Tornadoes

JOSHUA WURMAN

Center for Severe Weather Research, Boulder, Colorado

CURTIS R. ALEXANDER

School of Meteorology, University of Oklahoma, Norman, Oklahoma, and Center for Severe Weather Research, Boulder, Colorado

(Manuscript received 28 January 2004, in final form 2 July 2004)

ABSTRACT

A violent supercell tornado passed through the town of Spencer, South Dakota, on the evening of 30 May 1998 producing large gradients in damage severity. The tornado was rated at F4 intensity by damage survey teams. A Doppler On Wheels (DOW) mobile radar followed this tornado and observed the tornado at ranges between 1.7 and 8.0 km during various stages of the tornado's life. The DOW was deployed less than 4.0 km from the town of Spencer between 0134 and 0145 UTC, and during this time period, the tornado passed through Spencer, and peak Doppler velocity measurements exceeded 100 m s^{-1}. Data gathered from the DOW during this time period contained high spatial resolution sample volumes of approximately 34 m $\times$ 34 m $\times$ 37 m along with frequent volume updates every 45–50 s.

The high-resolution Doppler velocity data gathered from low-level elevation scans, when sample volumes are between 20 and 40 m AGL, are compared to extensive ground and aerial damage surveys performed by the National Weather Service (NWS) and the National Institute of Standards and Technology (NIST). Idealized radial profiles of tangential velocity are computed by fitting a model of an axisymmetric translating vortex to the Doppler radar observations, which compensates for velocity components perpendicular to the radar beam as well as the translational motion of the tornado vortex.

Both the original single-Doppler velocity data and the interpolated velocity fields are compared with damage survey Fujita scale (F-scale) estimates throughout the town of Spencer. This comparison on a structure-by-structure basis revealed that radar-based estimates of the F-scale intensity usually exceeded the damage-survey-based F-scale both inside and outside the town of Spencer. In the town of Spencer, the radar-based wind field revealed two distinct velocity time series inside and outside the passage of the core-flow region. The center of the core-flow region tracked about 50 m farther north than the damage survey indicated because of the asymmetry induced by the 15 m s^{-1} translational motion of the tornado. The radar consistently measured the strongest winds in the lowest 200 m AGL with the most extreme Doppler velocities residing within 50 m AGL. Alternate measures of tornado wind field intensity that incorporated the effects of the duration of the extreme winds and debris were explored. It is suggested that damage may not be a simple function of peak wind gust and structural integrity, but that the duration of intense winds, directional changes, accelerations, and upwind debris loading may be critical factors.

1. Introduction

Damage surveys depend upon the existence of damage indicators along with knowledge about their structural integrity, which is often difficult to discern when the damage is extreme (Marshall 1992, 2002). Other complicating factors include variations in both the upwind debris load from adjacent structures and the duration of damaging wind speeds. Radar-measured Doppler velocities also have inherent biases when used to estimate tornado wind speeds. Doppler velocity measurements are biased toward the motion of more reflective, usually larger, objects in sample volumes. Therefore, in regions where large debris becomes entrained in the tornado's circulation, Doppler velocities are predominantly measuring debris motion (Dowell et al. 2001, 2005, hereafter DAWW), not air motion. This is especially problematic considering that both inertial and drag forces generally increase with larger objects and result in larger departures from surrounding air motion.

Given the inherent errors in using either damage surveys or Doppler velocities to estimate tornado intensity, accurately assessing tornado intensity can be very difficult. There is a need to establish an accurate tornado climatology across the United States in order to better understand the temporal and spatial distributions of

Corresponding author address: Joshua Wurman, Center for Severe Weather Research, 1945 Vassar Circle, Boulder, CO 80305.
E-mail: jwurman@cswr.org

weak, strong, and violent tornadoes (Doswell and Burgess 1988). An accurate tornado climatology provides analog events that can be operationally used to forecast future severe weather events, and the climatology yields an assessment of regional hazards.

Gauging tornado intensity is also important from a structural engineering standpoint. Accurate observations of tornado wind speeds and resulting structural damage could improve engineering simulations of progressive structural failure and ultimately result in the design and construction of safer, more secure buildings (Mehta 1976; Marshall 1983, 1992). There are multidisciplinary efforts underway to revise the Fujita scale (F-scale) by improving the correlation between damage and intensity, especially in regions where there are few if any damage indicators (Marshall 2004). Detailed comparisons of tornado damage and Doppler velocity measurements are likely to improve tornado climatologies and structural engineering designs, and to assist efforts to enhance the Fujita scale to make it an even more useful tool for estimating tornado intensity.

Until the late 1990s, high-resolution observations of tornadoes from mobile radars were confined to rural areas where the was a paucity of observed damage (Bluestein et al 1995; Bluestein and Pazmany 2000; Wurman et al. 1996a,b, 1999). Distribution of observed damage was insufficient to permit a meaningful comparison with the high-resolution Doppler velocity data. However, on the evening of 30 May 1998, a supercell moved across southeastern South Dakota and produced a large and violent tornado that passed through the town of Spencer. The structural evolution of this tornado was detailed in the first part of this study (Alexander and Wurman 2005, hereafter Part I). A Doppler on Wheels (DOW) mobile radar (Wurman et al. 1997; Wurman 2001) was positioned a few kilometers away from the tornado and Spencer (Fig. 1), and the radar measured, at high-resolution, Doppler velocities across the tornado vortex before, during, and after the tornado passed through Spencer (Fig. 2). The core of the tornado passed through the south-central portion of the town, and this resulted in significant and widespread property damage along with the loss of six lives. While the loss of life and property was tragic, the high density of structures in the town provided sufficient coverage for the first meaningful comparison between damage distribution and radar-observed wind velocities.

The town of Spencer covers an area approximately 1 km $\times$ 1 km, with most building structures confined to within about 10 m AGL. A typical building lot had dimensions on order of 25 m $\times$ 50 m (1.2×10^3 m^2). The scanning strategy employed by DOW3 consisted of rotating the antenna at about 30° s^{-1} across 140° sectors with a PRF of 4000 Hz, using 64 pulses per integration, and a pulse width of 37 m. This produced nearly symmetric oversampled volumes across the town of Spencer with projected footprints of 34 m $\times$ 37 m (1.1×10^3 m^2). Thus there was very nearly one radar observation per structure. There were usually 6–10 elevation angles per volume ranging from 0.5° to 18° with spacing about every 1°–2°, and this resulted in sample volume updates every 45 s. The Weather Surveillance Radar-1988 Doppler (WSR-88D) at Sioux Falls, South Dakota (KFSD), running the volume coverage pattern 11 (VCP11) scanning strategy produced sample volumes with projected areas of 1285 m $\times$ 250 m (3.2×10^5 m^2) corresponding roughly to one-half the area of the entire town of Spencer and sample volume updates every 300 s (Table 1). It is critical to note that the DOW radar observations, while at an unprecedented low altitude (as low as 20–30 m AGL), were still significantly above building height (0–10 m AGL).

2. Damage survey

a. Fujita scale

Letzmann (1923; see also Peterson 1992a,b), Fujita (1971, 1973, 1992), and Fujita and Smith (1993) examined numerous damage paths from tornadoes across the United States and Europe. The F-scale wind speed was defined as the fastest quarter-mile of wind at any one location (McDonald 2001). By this definition, about 22 s of 18 m s^{-1} winds were necessary to meet the F0 criteria, decreasing to slightly over 3 s of 117 m s^{-1} winds to attain an F5 rating. These winds were defined at typical structural heights. (In Spencer typical structures occupied 0 to 10 m AGL, with the water tower extending to approximately 30 m AGL).

b. Damage in Spencer

Extensive ground and aerial photographs of Spencer were taken during the two days after the tornado passed through the town. Aerial and ground damage surveys were completed by the National Weather Service (NWS) and the National Institute of Standards and Technology (NIST). While an independent F-scale estimate for each structure was desired for comparison with the radar data, this was not established by the official damage survey. Only an overall peak intensity rating of F4 was assigned to the tornado. The photographic documentation along with notes provided by damage survey team members from NIST were the basis for the F-scale ratings assigned to every structure used in this comparison (L. Phong and B. Smith 2002, personal communication). The F-scale rating assigned to each damaged building was adjusted based on structural integrity (Fujita 1992). The distance between dwellings of 25 to 50 m acted as a practical limit on the resolution of the F-scale damage survey.

The aerial photographs of the damage in Spencer, when compared to the interpolated path of the velocity couplet's center, made clear that significant structural damage (F2 or higher) only extended about 100 to 150 m north of the center's track (Fig. 3a). To the south of the

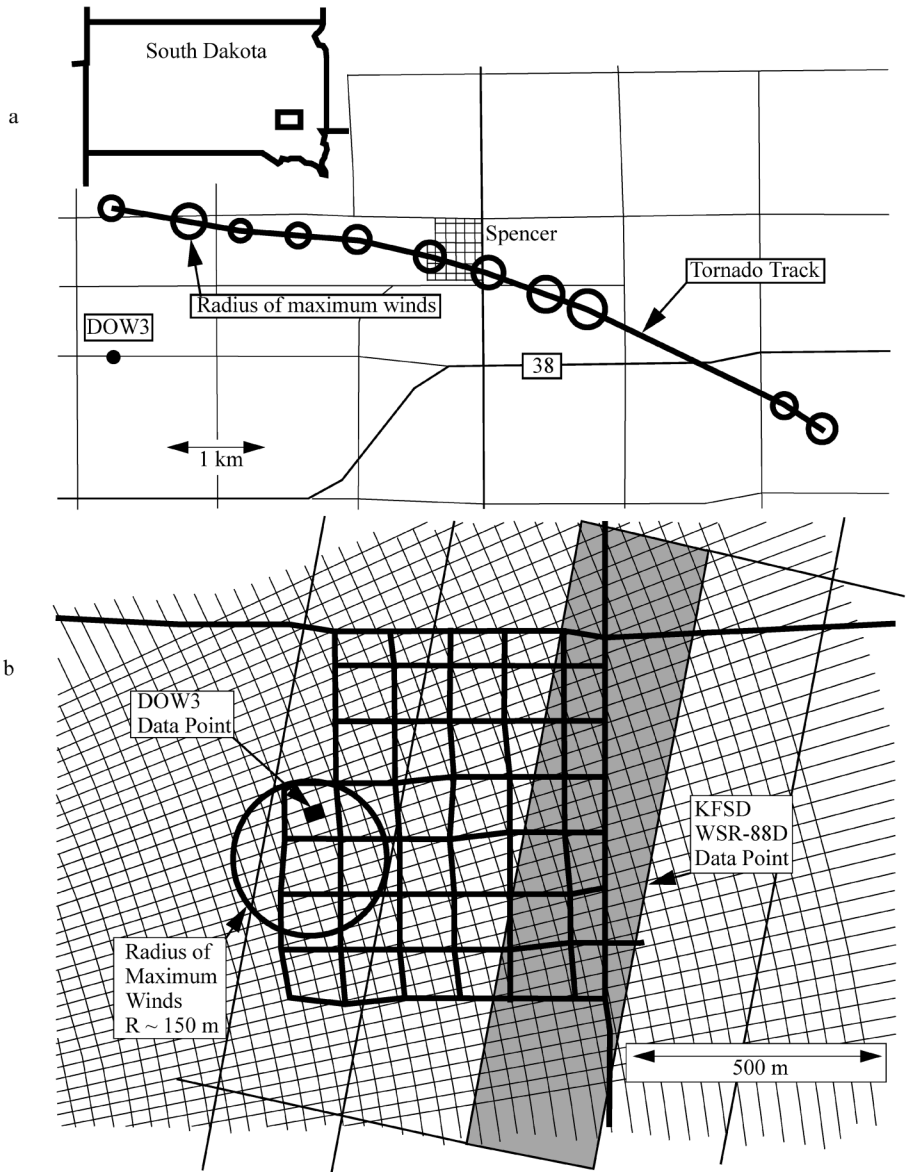

FIG. 1. Geometry of the DOW radar deployment showing geographic locations of (a) the tornado core-flow region, DOW3, and Spencer, SD, between 0134 and 0145 UTC 31 May 1998 and (b) the polar grid of radar data samples from both DOW3 and KFSD over the street map of Spencer. The position and size of the tornado's core-flow region at 0138:29 UTC is shown for reference.

track, significant damage was observed outward to between 200 and 250 m (Fig. 3b). NIST survey members noted that the path width of near total destruction was approximately 275 m, while the affected area path width appeared to be almost 800 m. In contrast, the width of the core-flow region in the tornado vortex was approximately 350 m as viewed by DOW3 when the tornado was passing through Spencer (Part I). The narrowness of the swath of most intense damage compared to the tornado's observed core-flow diameter may have been due to inward tapering of the tornado between the lowest observed level, near 30 m AGL, and building height, 0–10 m, as discussed later.

Along and north of the track centerline, F-scale ratings mostly ranged from F0 to F2, while south of the track the ratings ranged from F0 to F4 (Fig. 4). Many of the structures in Spencer were either weak frame houses or strong outbuildings, as categorized by the modified Fujita scale (Fujita 1992). This evaluation was conducted by the authors based on post-tornado photographs. This structural classification resulted in a reduction of initial F-scale estimates by one, two, or even three categories. The apparent asymmetry in damage across the track of the tornado was consistent with higher Doppler velocities measured on the south side of the tornado vortex. The velocity differential would result

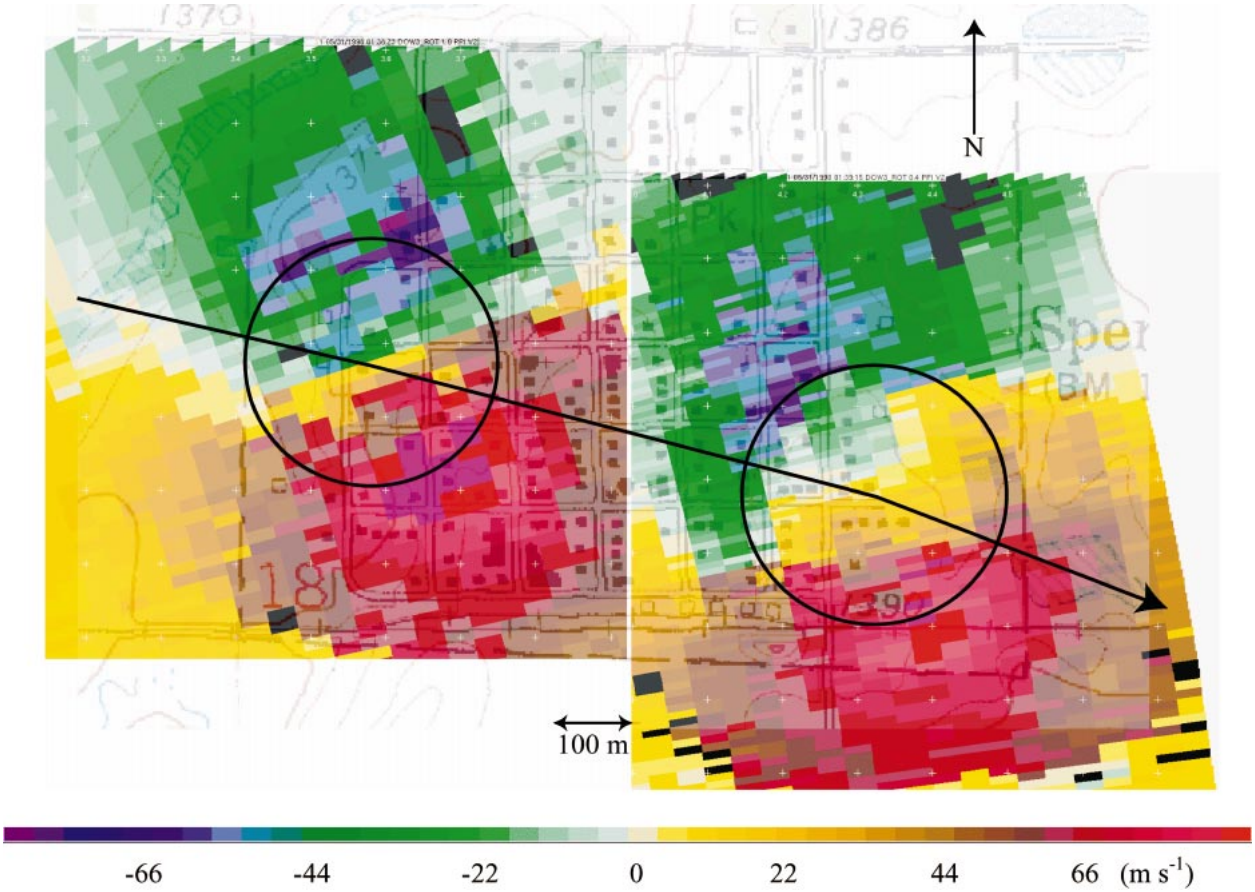

FIG. 2. Doppler velocity field (m s^{-1}) over the Spencer town map showing the consecutive 0.5° elevation scans centered around (left) 0138:29 and (right) 0139:18 UTC. The centerline of the radar beam is at an elevation of approximately 30 m AGL. The interpolated path of the vortex center and radius of maximum Doppler velocities are also shown (black). The magenta gates indicate Doppler velocities in excess of 93 m s^{-1}.

in wind speeds nearly 30 m s^{-1} higher on the south side of the tornado, which would translate to a difference of about 1.5 F-scale categories in areas that experience significant damage.

3. Radar-constrained tornado model

a. Maximum wind speed

Using the conceptual model of an axisymmetric vortex that is translating, an estimate of the peak rotational velocity in the tornado vortex was determined. It was necessary to account for the observation angle of the radar relative to the direction of tornado translation. The radar measured the peak outbound (or inbound) Doppler velocity (V_d) at an elevation angle (ϕ), azimuth angle (θ), and range (r) from the radar, where all angles are measured clockwise from due north except the elevation angle. It is important to note that it is assumed herein that V_d represents the Doppler velocity of air, neglecting centrifuging effects (DAWW). Relative to the center of the velocity couplet, the position of the maximum Doppler velocity measurement was at a vortex angle (α), while the centroid of the couplet had a heading (β) and speed (V_t) that was based upon linear interpolation of the centroid position between successive radar volumes (Fig. 5). This yielded an analytic function for the maximum rotational speed (V_{rm}) of the tornado,

$$V_{rm} = \frac{V_d \sec\phi - V_t \cos(\beta - \theta)}{\sin(\alpha - \theta)}. \qquad (3.1)$$

When considering very low elevation angles around 0.5°, and that the maximum Doppler velocities were nearly always measured at points where the radar beams were tangent to the tornado vortex, this analytic function can be approximated by

$$V_{rm} \approx V_d - V_t \cos(\beta - \theta), \qquad (3.2)$$

where the maximum outbound (or inbound) Doppler velocity has the component of translation removed from the measurement to provide an estimate for the maximum rotational velocity (peak tornado-relative wind speed). As an estimate of the error produced by this approximation, taking typical values of $V_d = 90$ m s^{-1}, $V_t = 15$ m s^{-1}, $\phi = 1.0$, $(\beta - \theta) = 180°$, and an extreme

TABLE 1. Radar characteristics and scanning strategies.

Parameter	DOW3	KFSD WSR-88D
Wavelength (cm)	3.2	10.0
Beamwidth (°)	0.93	1.0
Antenna rotation rate (°s^{-1})	30	20
Pulse repetition frequency (Hz)	4000	1013
Hits per dwell	64	52
Oversampling factor	2	1
Half-Nyquist interval (m s^{-1})	32	25
Range to Spencer (km)	4	71.5
Beam height at 0.5° over Spencer (m)	30	925
Range gate size (m)	37	250
Volume resolution over Spencer (m)	34 × 34 × 37	1285 × 1285 × 250
Projected area of samples over Spencer (m^2)	1.1×10^3	3.2×10^5
Volume update period (s)	45	300

case where $(\alpha - \theta) = 70°$ indicating that the peak Doppler velocity is 20° from a point on the vortex that was tangent to the radar beam, the result using (3.1) is 112 m s^{-1} while the value from (3.2) is 105 m s^{-1}, producing a relative error of about 6%.

This analysis produced two estimates for the maximum rotational velocity based upon the maximum inbound and outbound Doppler velocities. In a purely axisymmetric vortex, the two Doppler velocities would yield the same result for the peak rotational velocity. In the Spencer tornado, perturbations in the tornado wind field, possibly caused by multiple vortices, often resulted in significantly different estimates for the peak rotational speed (Wurman 2002; Part I; Lee and Wurman 2004, manuscript submitted to *J. Atmos. Sci.*). The mean of the two estimates was used as the peak rotational velocity for each radar volume.

DOW resolution volumes were small, *O*[40 m], and the winds in the tornado were quite intense *O*[100 m s^{-1}]. Therefore, individual mean Doppler measurements represented parcels that crossed individual locations in less than 1 s. Sub-radar-resolution-scale gusts, which might be estimated from spectral width data, would have persisted for tenths of seconds and were neglected in this study.

b. Tornado cross sections

After establishing an estimate of the peak wind speed in the tornado, it was useful to extend the analysis of the wind field from the one-dimensional point measurements to a more complete two-dimensional description of the tornado wind field within 50 m AGL, and to include the evolution of this peak wind speed, the core-flow diameter, and the translational motion of the vortex. However, since only single-Doppler data were available for this case, it was again necessary to assume an axisymmetric translating vortex and examine several cross sections through the tornado while using the conceptual model to account for the components of rotation and translation not observed by the radar (Fig. 5). Several horizontal cross sections through the centroid of the velocity couplet were compared with best-fit lines to establish a two-dimensional radar-constrained model of the tornado wind field (Wurman and Gill 2000; Wurman 2002). The cross sections were taken along an axis at a constant range from the radar producing an azimuthal arc through the center of the rotational velocity couplet. This cross section was preferred over a straight line through the tornado because at close range to a large vortex, the radar samples the largest component of the tornado wind field along an azimuthal arc through the center of the vortex. The best-fit lines were based upon the established conceptual model where two unique flow regions were identified from the Doppler velocity data in the cross sections (Fig. 6). In the region between the center of the velocity couplet and the radius of highest Doppler velocities (R), hereinafter referred to as the core-flow region, the profile of Doppler velocities closely matched that of solid-body rotation. In the region outside of the radius of highest Doppler velocities, the Doppler velocities decayed exponentially away from the core flow at approximately a rate of $D^{-0.67}$. This horizontal wind profile both inside and outside of the tornado's core appeared very consistent with the structure of other large and violent tornadoes (Wurman 1999, 2002; Wurman and Gill 2000).

Therefore, the horizontal wind speed (V_h) at any horizontal distance (D) and direction (α) from the center of the velocity couplet was described by

$$V_h = [V_t^2 + V_r^2 + 2V_tV_r \sin(\alpha - \beta)]^{0.5}, \quad (3.3)$$

where

$$V_r = V_{\rm rm}\frac{D}{R} \qquad \text{when } D \le R, \quad (3.4)$$

$$V_r = V_{\rm rm}\left(\frac{R}{D}\right)^{0.67} \qquad \text{when } D \ge R. \quad (3.5)$$

Velocity cross sections through the tornado wind field were constructed for all 11 volume scans using the lowest-level radar scans, and while perturbations existed in the Doppler velocity field for each volume, the slope of the velocity profile both in the core region and outside

FIG. 3. Aerial photographs of the tornado damage in Spencer showing (a) the north side and (b) the south side of the damage track. The cyan arrow represents the interpolated path of the Doppler velocity couplet center based on DOW radar data (courtesy of B. Smith).

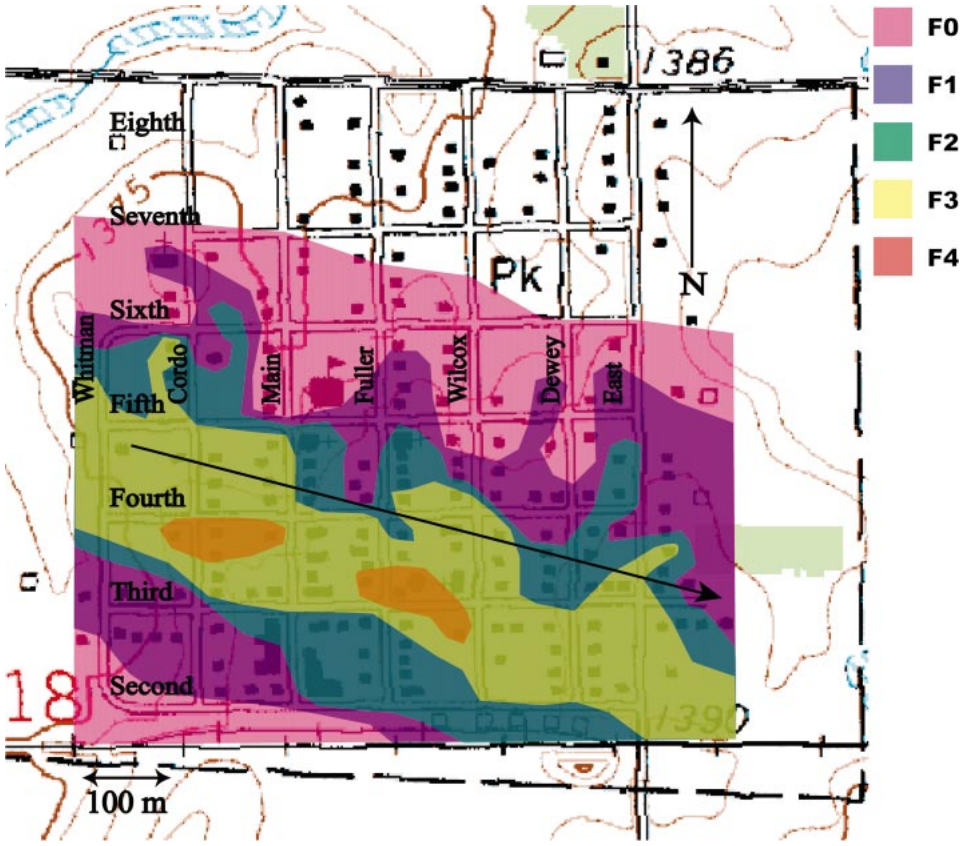

FIG. 4. Damage F-scale ratings (F_D) for all structures in Spencer based upon damage photography, structural integrity, and damage survey field notes. Some detail is not shown for clarity. The long black arrow represents the interpolated path of the Doppler velocity couplet center.

the core flow consistently followed solid-body rotation and a 0.67 exponential decay, respectively. Occasionally it was not possible to extend an azimuthal cross section through both the center of the couplet and one or both velocity maxima because of a small divergent component present in the velocity couplet possibly due to debris centrifuging (Zrnić et al. 1985; Dowell et al. 2001; DAWW). It is also possible that weak multiple-vortex structure complicated the axisymmetric assumptions inherent in this process (Part I). Nevertheless, the slopes of the Doppler velocities across the core-flow and decay regions remained consistent between volume scans. The fact that the flow outside the core exhibited a decay rate less than $1/R$ is evidence of frictional loss of angular momentum. (Parcels spiraling inward toward the core-flow region without losing angular momentum would exhibit wind speed increases proportional to $1/R$.)

For each 0.5° elevation scan through the tornado, a new maximum rotational velocity (V_{rm}), core radius (R), translational speed (V_t), and direction of movement (β) were calculated. Since the time between consecutive 0.5° elevation scans was usually around 45 s, it was necessary to interpolate the peak rotational velocity (V_{rm}) and radius of core flow (R) between the scans, while keeping the translational speed and direction constant between volumes.

The assumptions in this radar-constrained model of the wind field include an axisymmetric vortex structure with no radial component to the flow other than that induced by translation of the vortex. Some numerical and laboratory modeling results indicate that at or above the top of the surface inflow layer, usually found to be around 30 m AGL, the radial component of the vortex flow was very small while vertical air motions in this region were found to be quite significant, near 50 m s^{-1} (Lewellen et al. 1997). While neglecting radial flow appears justified, vertical air motions were not measured by the radar at 0.5° elevation and were not included in this model. Given the paucity of detailed observations in the lowest levels of tornadoes, it is difficult to fully evaluate the validity of the model's simplifications.

Given the spatial and temporal resolution of the radar data, and the resulting model wind field, an arbitrary time step of 1 s and a horizontal grid spacing of 10 m were selected to generate a Cartesian grid for the wind speed field across the 1 km × 1 km domain over the town of Spencer. The tornado wind field was calculated for every second between 0134:27 and 0144:57 UTC (Fig. 7).

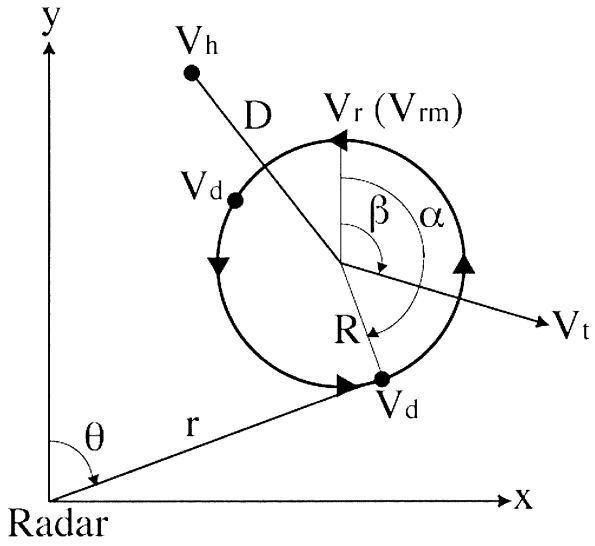

FIG. 5. Schematic representation of the geometry used to estimate the maximum rotational velocity of the tornado vortex. The maximum inbound and outbound Doppler velocities (V_d) are located at a range (r), azimuth (θ), and elevation (ϕ) relative to the radar, and at a range (R) and azimuth (α) relative to the center of the tornado vortex. The center of the tornado vortex has a translational azimuth (β) and speed (V_t). The estimated maximum rotational speed (V_{rm}) is also located at a range (R) relative to the vortex center. The estimated total horizontal wind speed (V_h) at any distance (D) relative to the center of the tornado is based upon the vector sum of the translational and rotational wind vectors.

4. Comparison of model and damage F-scales

a. Model parameters

The radar-constrained wind speed model of the Spencer tornado revealed that the tornado's center took approximately 60 s to cross the town after entering the west side just south of Fifth Street, exiting the east side just north of Third Street. The most extensive damage appeared to be located between Second and Fourth streets primarily on the south side of the tornado's path (Fig. 4). The official damage survey placed the center of damage path about 50 to 75 m farther south. The radar-constrained model also revealed that it took nearly 300 s for the potentially damaging effects of the tornado's wind field to pass through the entire town.

Fujita's (1971) decision to relate damage intensity to what is effectively the peak wind gust was somewhat arbitrary. An argument can be made that damage to structures can occur from either peak over pressures (which are highly correlated with peak wind gusts) or from the accumulated and stochastic effect of debris impacts (which are correlated to both wind speed and intense wind duration), or by a complex combination of both effects. It is also plausible that structural integrity may be impacted by winds that vary rapidly in intensity. Furthermore, many structures are likely to exhibit variability in their susceptibility to intense winds emanating from different directions. Therefore a structure that experiences a wind gust of a certain magnitude from only one direction might be less likely to fail than the same structure if it experienced winds of the same magnitude but from multiple directions.

To explore the possible impact of intense wind duration, the accumulated effects of debris impacts, and abrupt changes in wind speeds, several alternate metrics of tornado damage potential, all derived from the radar-constrained model, were calculated.

1) HIGHEST WIND GUSTS AND F-SCALE

The conventional application of the Fujita scale is to associate observed damage with peak wind gusts. The highest 5-s average wind speed at each location on the grid revealed that a nearly 100-m-wide path between Third and Second Streets on the west side of the town experienced a 5-s average wind at or above 100 m s^{-1} (Fig. 8a). The highest 5-s average wind speed had a maximum of about 112 m s^{-1} on the western edge of town around Third Street. The highest 60-s average wind speed at each point in the town showed a 50-m swath across the south-central portion of the town between Second and Third Streets where this parameter reached a maximum of just over 80 m s^{-1} (Fig. 8b). Using Fujita's F-scale definition, the radar model calculated the fastest quarter-mile of wind at every location and associated these values with Fujita's F-scale ratings, hereinafter referred to as F_R (Fig. 8c). Not surprisingly, the peak quarter-mile wind speeds were nearly identical to the fastest 5-s average speed at each grid point. Note that subsecond wind gusts, capable of being estimated through single-radar-gate and spectral width data as discussed above, were not considered in this study.

The F_R was calculated at each grid point for comparison against the damage-based F-scale estimates hereinafter referred to as F_D (Fig. 8d). The F_R contours were very smooth, and their gradient across the town in either direction from the track of the tornado's center was considerably smaller than that of the F_D contours. Most structures received a higher F_R rating than F_D rating. The worst observed damage (highest F_D) was located approximately one-half block north (50 m) closer to the path of the tornado center than were the maximum F_R ratings. However, both rating systems had a maximum value in the F4 range. It is worthwhile to note that the observed asymmetric tornado contained ground-relative wind speeds as high as 118 m s^{-1}, slightly into the F5 range, as it passed over the western edge of the town.

The area that experienced high F_R was larger than the area that experienced high F_D, suggesting that significant debris centrifuging had spuriously increased the measured diameter of the core-flow region in the Doppler velocity field (Snow 1984; Zrnić et al. 1985; Dowell et al. 2001; DAWW). Navigation errors would have caused a shift north or south, rather than the observed expansion of F_R in both directions. Moreover azimuthal navigation errors were estimated to be on the order of

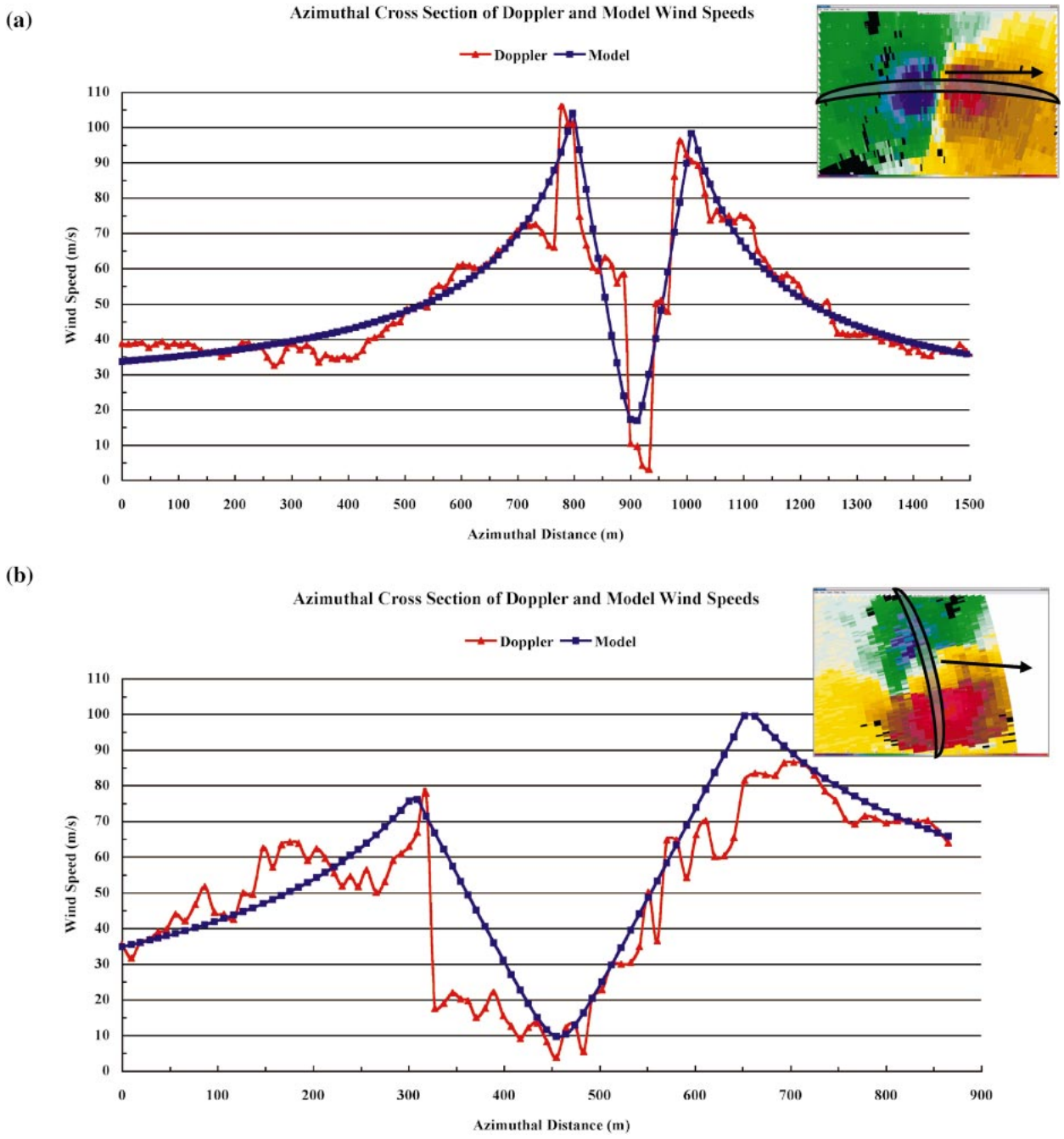

FIG. 6. Azimuthal cross sections through the core of the 0.5° elevation Doppler velocity couplets (red) and wind speeds from the axisymmetric vortex model (blue) at (a) 0134:30 UTC when the center of the tornado was 3.6 km west of Spencer, and (b) 0139:11 UTC when the tornado was 0.1 km east of Spencer. The insets show the location of the Doppler velocity cross section relative to the direction of tornado vortex translation.

only 0.1° (Part I), or less than 10 m over the town, much less than the observed 50-m offset between F_D and F_R. The radar reflectivity field in the lowest tilt of each volume over Spencer revealed a well-defined disk of high reflectivity values likely indicative of large debris. Higher-elevation scans did reveal reflectivity minima at the center of the vortex that may be an indication of the necessary debris residence time in the vortex updraft and inflow region before substantial centrifuging could be established (Dowell et al. 2001; DAWW). Another possible explanation for a portion of the 50-m offset is the difference between the level at which damage occurred (5 m AGL) and radar observation level (30 m AGL). Many tornadoes are observed to taper inward

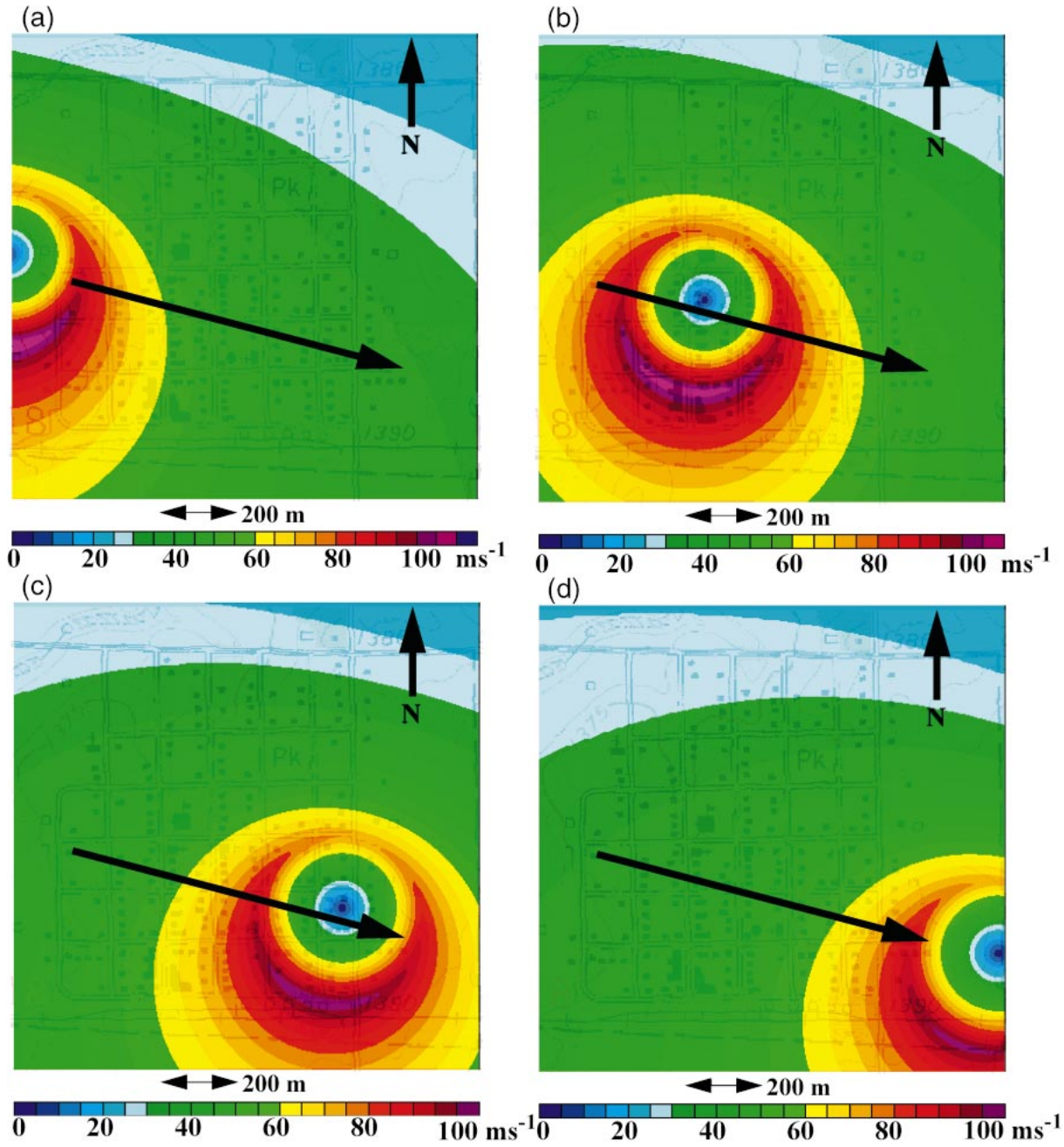

FIG. 7. The radar-constrained model showing the instantaneous wind speed (m s^{-1}) over the map of Spencer at (a) 0138:21, (b) 0138:45, (c) 0139:10, and (d) 0139:30 UTC. Interpolated track of tornado center is shown (black arrow).

near the ground (Wurman and Gill 2000; Part I; and many visual observations), as modeling studies have suggested (Lewellen et al. 1997), and the tornado wind field might have been narrowest very near the surface. A two-to-one inward tapering in the lowest 30 m AGL would be sufficient to account for the entire 50-m expansion of F_R compared to F_D. However, there are no confirming radar or other data to quantify or evaluate this effect. It may be that a combination of centrifuging and tapering effects are in play.

2) DURATION OF INTENSE WIND SPEEDS

It is likely that debris with increasingly damaging potential is lofted by winds of increasing intensity, that is, strong winds loft heavier, more damaging debris than weak winds. Therefore the duration of winds above certain thresholds would be an alternate measure of tornado damage potential. The duration of F1, F2, F3, and F4 intensity winds were calculated using the radar model (Fig. 9). F1-level winds occur for

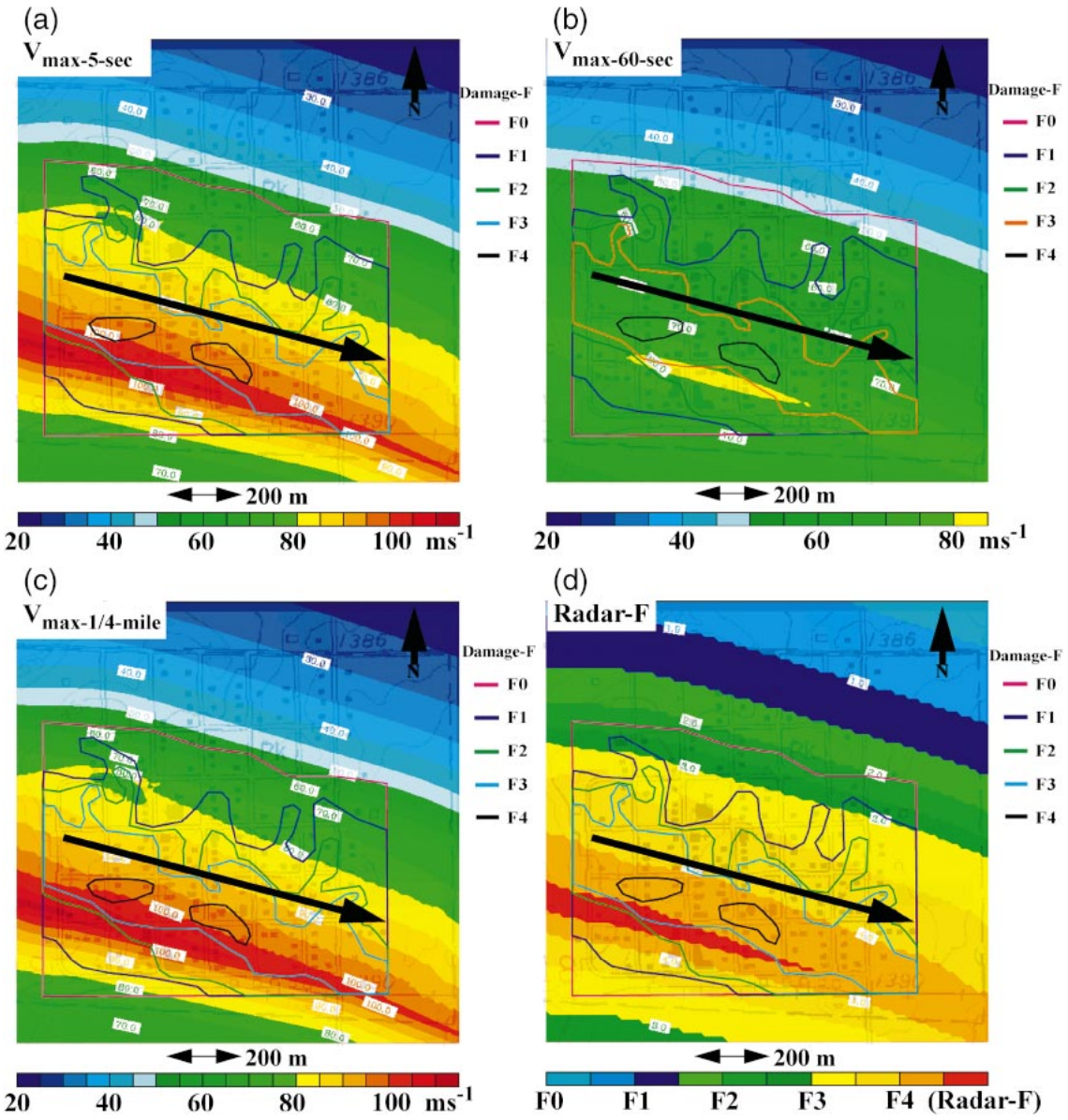

FIG. 8. Comparison between the damage F-scale ratings (F_D) (colored contours) and the (a) maximum 5-s average wind speed (m s^{-1}), (b) maximum 60-s average wind speed (m s^{-1}), (c) maximum 1/4-mile average wind speed (m s^{-1}), and (d) the radar-constrained model F-scale ratings (F_R) (color-filled contours) over the map of Spencer. Interpolated track of tornado center is shown (black arrow).

over 120 s well to the south of the tornado, and might be associated with F1-level damage, but there are insufficient damage indicators to the south of the town for a meaningful comparison. The duration of more intense winds—F2, F3, and F4—is shorter and is confined to a increasingly narrow swath to the south of the tornado track. F4-level winds occurred for a maximum time of 22 s in the southwest portion of the town, south of the F4 damage by approximately 50 m. The F4 wind duration track is quite similar to the peak wind gust tracks since the tornado did not vary significantly in intensity, size, or duration as it crossed the town. The location of the maximum duration of F4 winds is most closely related to the location of the most severe damage.

3) TIME-INTEGRATED WIND SPEED MOMENTS

In order to attempt to account for damage caused by not just the peak winds, but the integrated effect of all intense winds and associated lofted debris, wind swaths integrating wind speed (V), square of the wind speed (V^2), and cube of the wind speed (V^3) over time, using only winds speeds above 40 m s^{-1}, were calculated (Figs. 10a,b,c). As expected, the integrals of the higher powers of V were more narrowly distributed near the

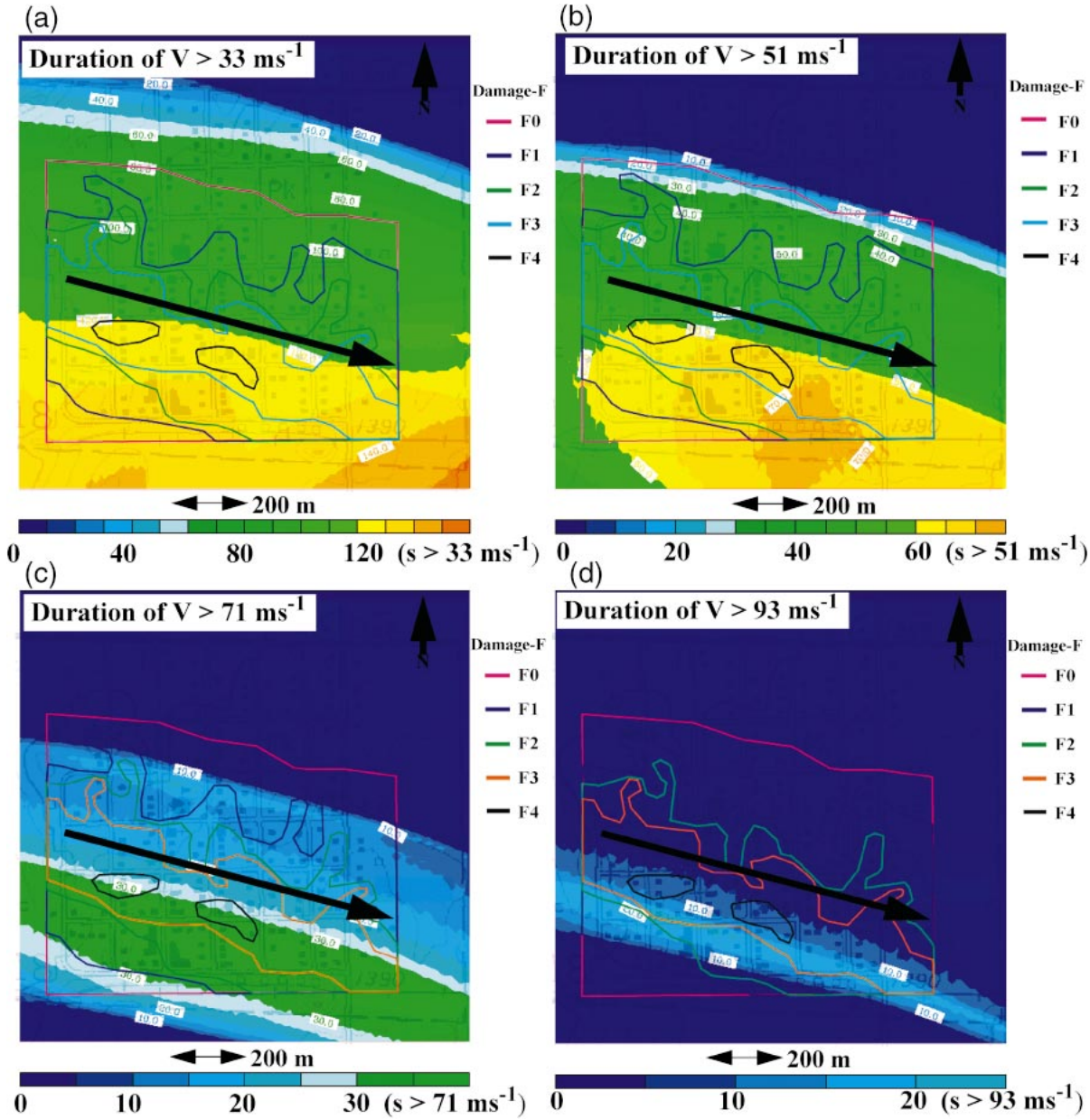

FIG. 9. Comparison between the damage F-scale ratings (F_D) (colored contours) and the duration of wind speeds (s) exceeding (a) 33, (b) 51, (c) 71, and (d) 93 m s^{-1}. Interpolated track of tornado center is shown (black arrow).

path of the peak winds and were more closely correlated to both the location, distribution, and extent of actual damage. However, the time integral of V was maximized on the east side of town while the most intense damage occurred well to the west. Since the kinetic energy and associated damage potential of lofted debris was likely to be proportional to higher powers of the wind speeds, the better correlation of the time-integrated V^2 (proportional to kinetic energy) and V^3 (crudely accounting for the increased kinetic energy of the debris and the dependence on wind speed of the typical mass of lofted debris) with observed damage was suggestive that the accumulated effects of debris impacts are important when assessing the damage potential of tornadoes.

4) ACCELERATIONS

Accelerations of the local airspeed near structures, at least by this tornado, did not seem to be well correlated with either the spatial extent or distribution of observed damage. The peak 1-s accelerations were near 10 m s^{-2} over the western portion of the town decreasing to about 8 m s^{-2} on the east side of town (Fig. 10d). All accelerations above 6.0 m s^{-2} were confined within the track

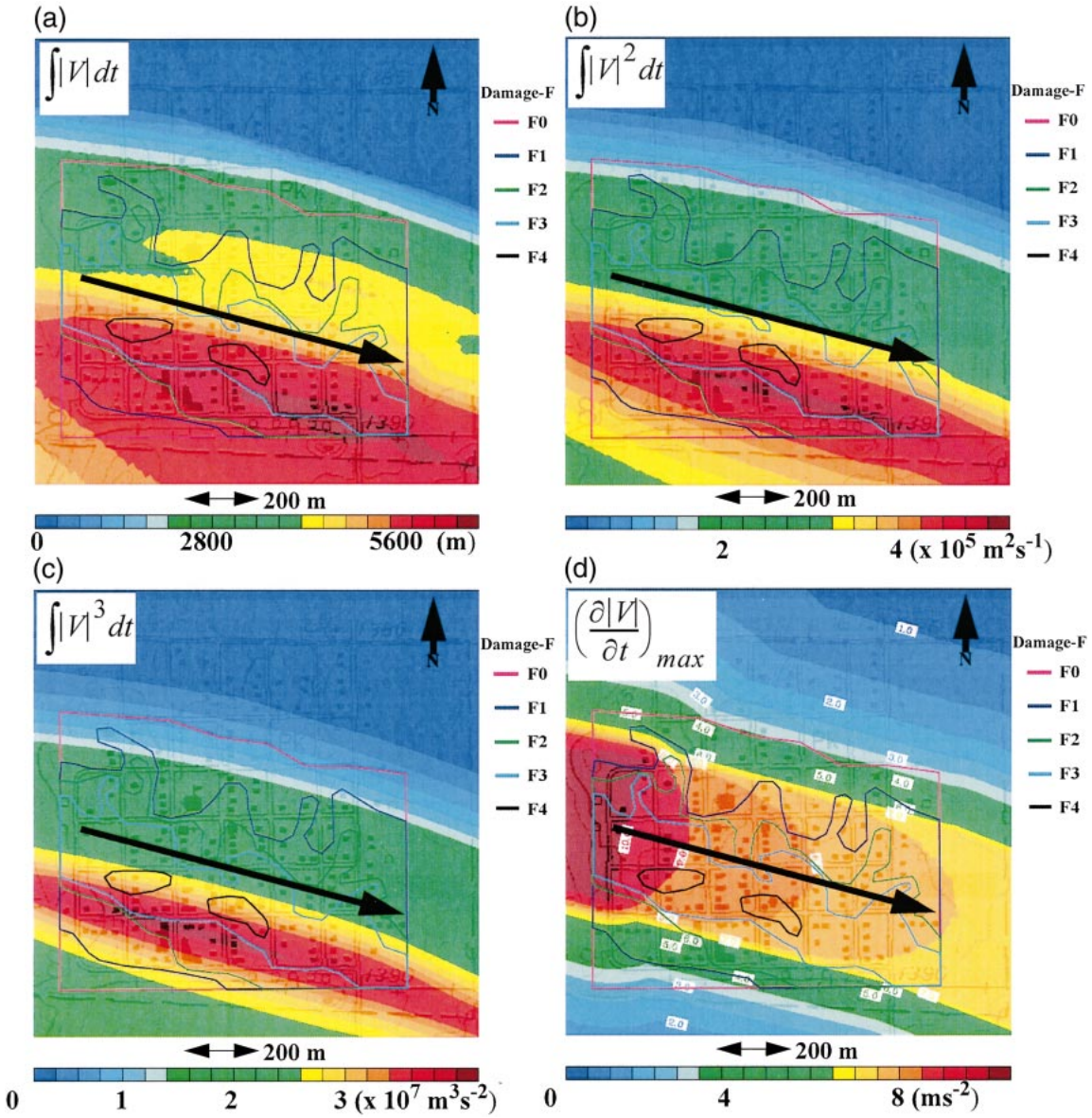

FIG. 10. Comparison between the damage F-scale ratings (F_D) (colored contours) and the (a) time-integrated wind speed (m), (b) time-integrated wind speed squared ($m^2\ s^{-1}$), (c) time-integrated wind speed cubed ($m^3\ s^{-2}$), and (d) the maximum 1-s wind acceleration ($m\ s^{-2}$). Only wind speeds above 40 $m\ s^{-1}$ are included in the time integrations. Interpolated track of tornado center is shown (black arrow).

of the core-flow region. It is important to note that significantly higher accelerations, up to 50 $m\ s^{-2}$, have been calculated in a different tornado containing multiple vortices (Wurman 2002).

b. *Comparison with NWS damage tracks inside and outside the town*

On a larger scale, F_R was compared with an NWS-produced F_D map (USDOC 1998). The model wind field was tracked across two 2.5 km × 2.5 km domains with a grid spacing of 20 m during the first two DOW observation periods between 0103 and 0122 UTC (Fig. 11), and an 8 km × 8 km domain with a grid spacing of 100 m for the final observation period from 0134 to 0145 UTC (Fig. 12). A 1-s time step was used for all model runs. The two F-scale ratings appeared very similar with the location, width, and intensity of the tornado tracks. However, during the early portion of the first observation period the F_R indicated the presence of an F1 tornado prior to any such observation in the F_D. The F_R was also one category higher than the NWS F_D just prior to and just after the time when the tornado was in Spencer. The F_R indicated a slow decrease in intensity

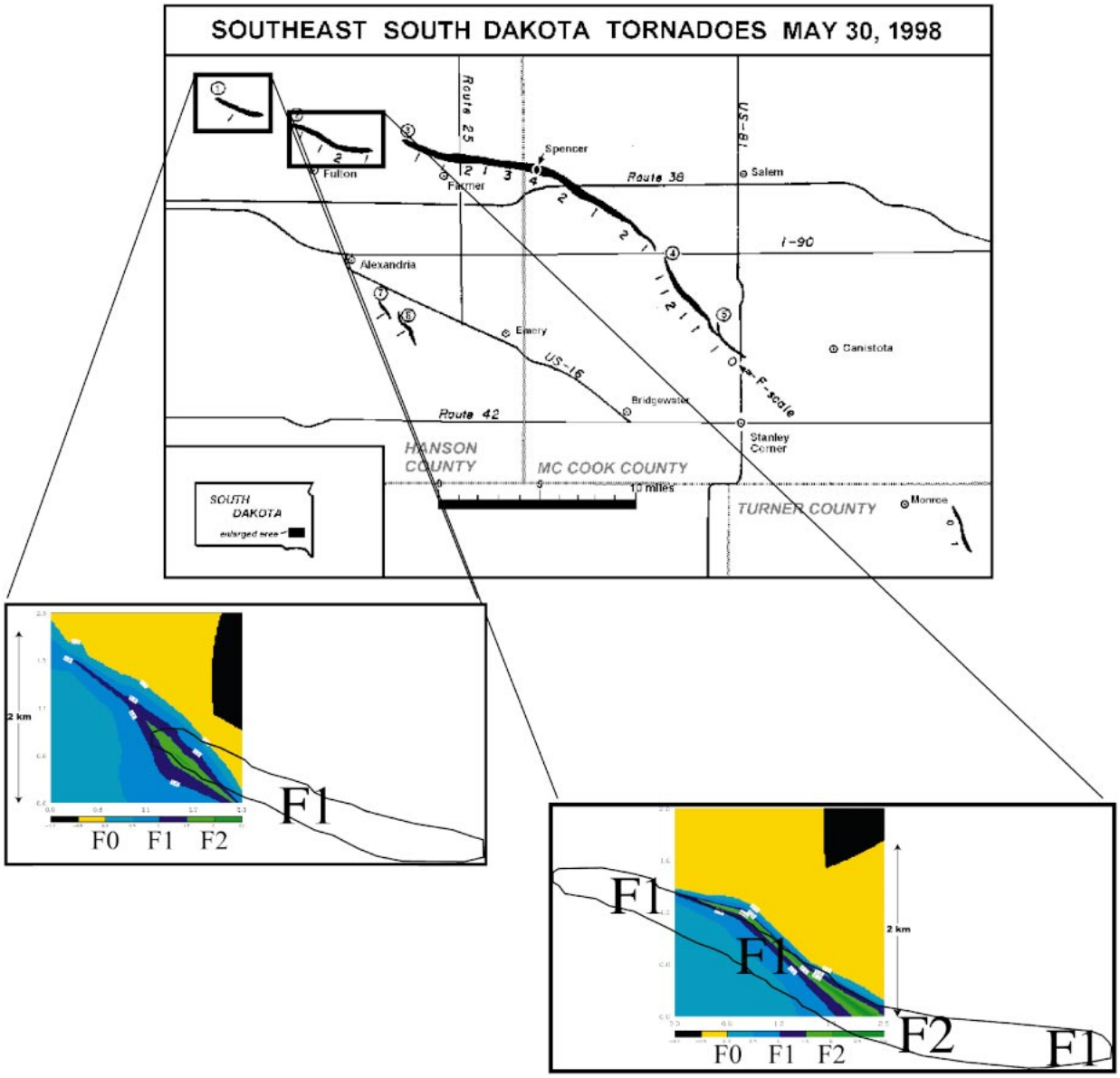

FIG. 11. A composite of tornado damage tracks based on aerial surveys (from USDOC 1998). (top) Relative path length, width, and damage F-scale ratings (F_D) are shown for all tornadoes and (bottom) the path segments where the radar-constrained model F-scale (F_R) was calculated from the first radar deployment site.

of the tornado starting just west of town, while not surprisingly the NWS F_D indicated much more abrupt transitions of intensity likely because of the absence of damage indicators outside of Spencer. The fact that F-scale ratings are dependent on the existence of damage indicators is well known (Doswell and Burgess 1988), but this is the first time that the discrepancy between observed tornado winds and damage has been quantitatively documented.

c. Time series over structures

Another comparison resulted from the generation of wind speed time series at specific grid points over Spencer that corresponded to the locations of significant structural damage. An exercise was conducted at a recent local severe storms conference where approximately 65 people were asked to assign F-scale ratings to specific structures in Spencer based upon a few damage photographs (Edwards 2003).

The most severe damage was observed at a crushed water tower that was composed primarily of steel and anchored into cement. The position of a damaged car on the crumpled water tower indicated the possibility that the car became a projectile that undercut the support beams of the tower (Fig. 13a). The official damage survey used this structural damage for the basis of the F4

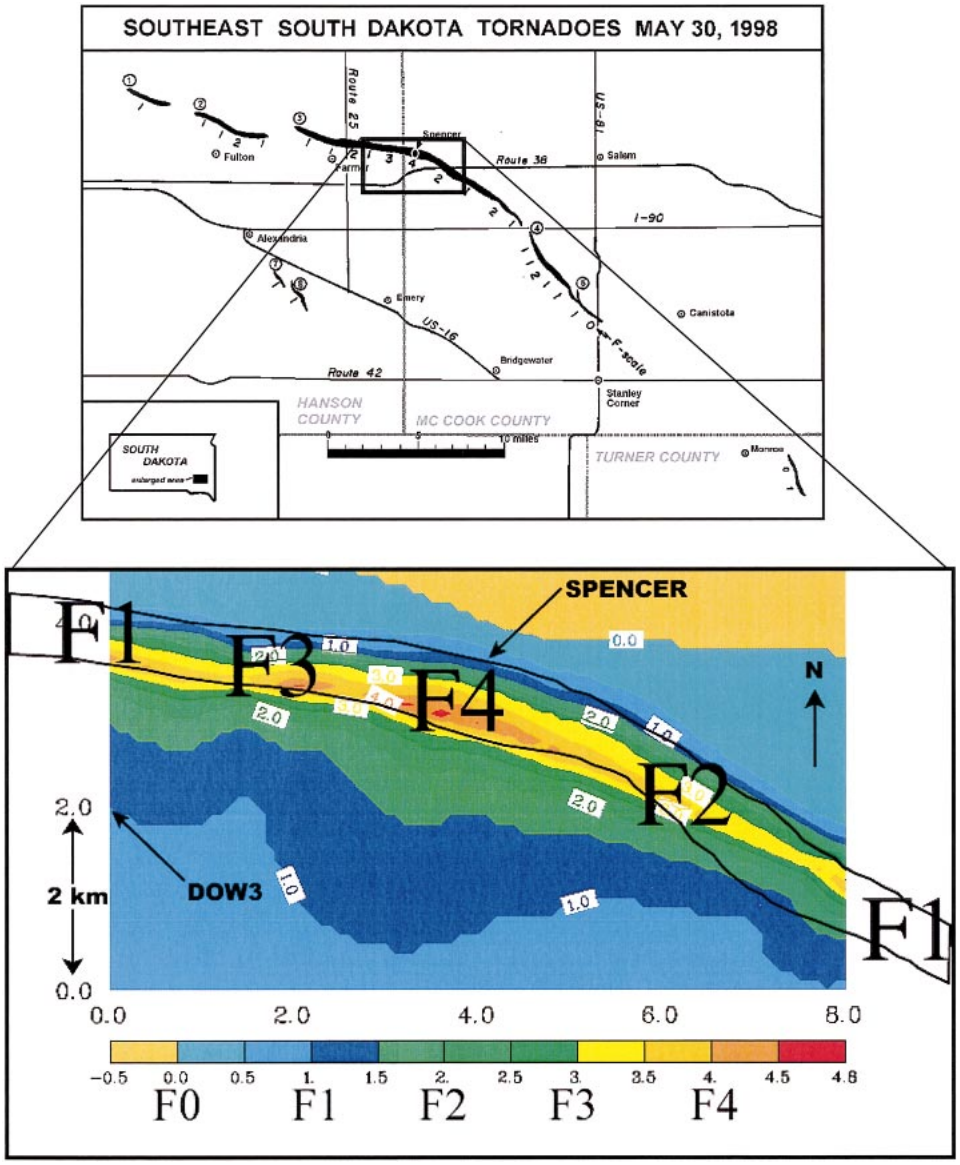

FIG. 12. A composite of tornado damage tracks based on aerial surveys (from USDOC 1998). (top) Relative path length, width, and damage F-scale ratings (F_D) are shown for all tornadoes and (bottom) the path segments where the radar-constrained model F-scale (F_R) was calculated from the second radar deployment site.

rating. The mean rating for this structure from people participating in the exercise was only F3.0. However, the standard deviation of these estimates was 0.8, or nearly an entire F category. The F_D from our study also yielded an F4 rating for this structure based upon the facts that the structure had collapsed and that it was classified as a strong frame house with no resulting compensation for the structural integrity (Fujita 1992). This structure experienced intense winds from two widely differing directions on each side of the core-flow region. It is likely that structural failure began after the impact of large debris (an automobile). Therefore, we speculate that had this structure experienced similar wind speeds, but from different directions, or only a single direction, and been missed by the automobile, it may not have collapsed. Furthermore, we speculate that some structures that are inherently less resistant to winds from certain directions (because of garage openings and bay windows) are more likely to suffer damage if subjected to intense winds from more than one direction.

The wind speed time series produced from the radar-constrained model at this location revealed two peaks in the wind speed (Fig. 13b), because the water tower was located 70 m south of the track of the tornado center well within the core-flow region. Wind speed accelerations in the core-flow region were around 8.0 m s^{-2} or about 0.8 g. These accelerations represented changes in the airspeed at particular locations and were not nec-

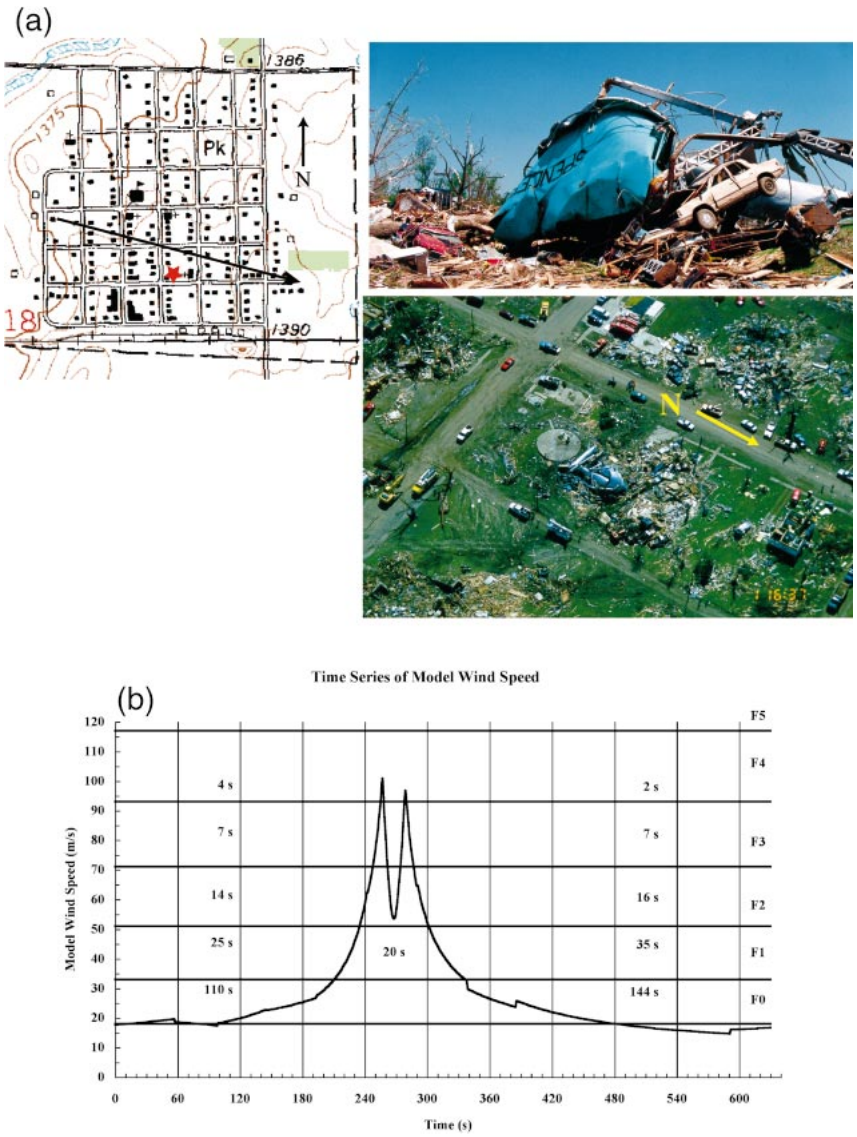

FIG. 13. F-scale comparison at the water tower located approximately 70 m south of the tornado track including (a) ground and aerial damage photography, which provided a damage F-scale estimate of F4, and (b) a time series of the radar-constrained model wind speed (m s^{-1}) at the nearest grid point over this structure (aerial photograph courtesy of B. Smith). The time duration of wind speeds in each F-scale category is shown for reference.

essarily representative of larger debris motion or actual air parcel accelerations in any Lagrangian sense. The wind speed peaked in the F4 range for durations of 4 and 2 s, respectively, and reached a maximum of 101 m s^{-1}, while remaining in or above the F2 range for a total of 70 s.

Another location of significant damage was an apartment complex located about one and a half blocks west of the water tower and about 130 m south of the track of the tornado center (Fig. 14a). This structure was rated with a mean of F3.0 by people participating in the exercise. Again, there was considerable disagreement among the participants, with a standard deviation of the F rating at 0.6. This complex was also classified as a strong frame house, and given the collapse of the roof and several interior walls, the building was judged to have experienced F3-level damage.

According to the radar model, the grid point over this structure received wind speeds in the F4 range for durations of 8 and 7 s, with a maximum speed around 105 m s^{-1} during both peaks (Fig. 14b). This location was very close to the radius of maximum winds at the closest approach of the tornado, and this resulted in a longer period of higher winds with little reduction of the flow in the core. The wind speed remained in the F2 or higher range for a total of 68 s.

A third structure used in the F-scale exercise was a set of grain-storage silos on the extreme south side of

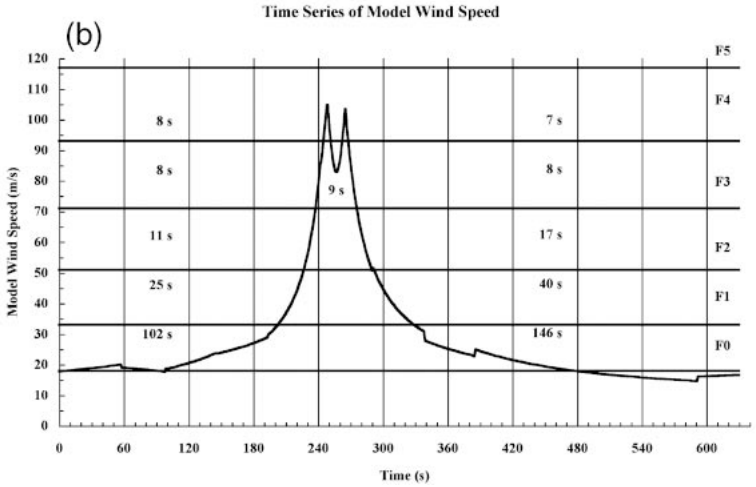

FIG. 14. F-scale comparison at the apartment complex located approximately 130 m south of the tornado track including (a) ground and aerial damage photography, which provided a damage F-scale estimate of F3 (courtesy of R. Edwards and B. Smith), and (b) a time series of the radar-constrained model wind speed (m s^{-1}) at the nearest grid point over this structure. The time duration of wind speeds in each F-scale category is shown for reference.

the town along Second Street (Fig. 15a). These silos were located approximately 220 m south of the tornado track and remained outside of the core-flow region as the tornado passed. In the exercise this structure was given a mean rating of F2.2 with a standard deviation of 0.8. This was a thin metal structure that was likely susceptible to debris penetration. Given this, the building was classified as similar to a weak frame house, and while the removal of the roof and partial collapse of the walls warranted an initial damage rating of f3, the structural integrity penalty resulted in a final damage rating of F2 herein. At the grid point closest to this location, the wind speed monotonically increased and then decreased, reaching a maximum value of about 93 m s^{-1} for about 6 s, with wind speeds in or above the F2 category for a total of 74 s (Fig. 15b).

Two other structures located on the north side of the tornado track near the eastern edge of Spencer were not rated in the damage survey exercise. However, there was a significant difference in damage severity between the two structures despite similar wind speed time series. The first structure was a mobile home located about 130 m north of the tornado track and inside the core flow region as the vortex reached its closest approach (Fig.

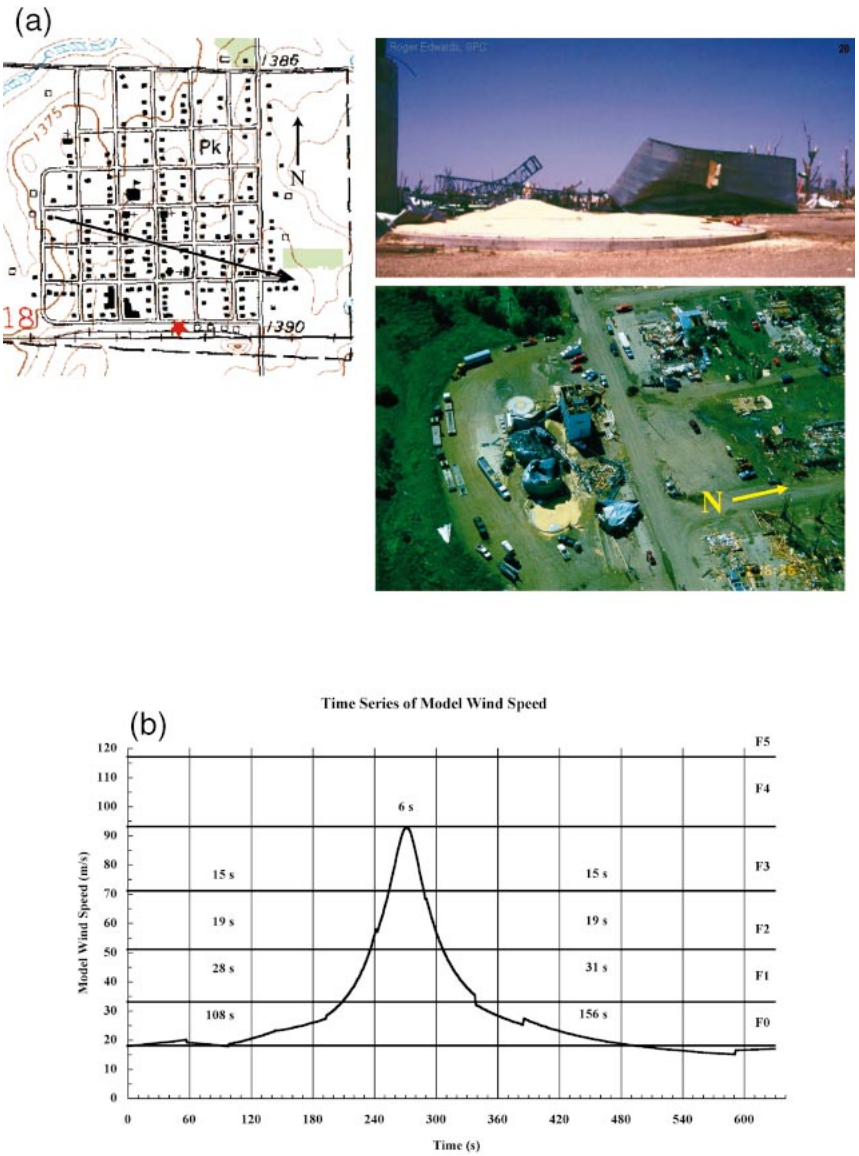

FIG. 15. F-scale comparison at the grain storage bins located approximately 220 m south of the tornado track including (a) ground and aerial damage photography, which provided a damage F-scale estimate of F2 (courtesy of R. Edwards and B. Smith), and (b) a time series of the radar-constrained model wind speed (m s^{-1}) at the nearest grid point over this structure. The time duration of wind speeds in each F-scale category is shown for reference.

16a). This location resulted in a wind speed time series similar to that over the water tower. However, peak winds on the north side of the tornado track were significantly lower than those on the south side because of the translation of the vortex. The time series associated with the mobile home's location peaked at 81 m s^{-1}, and remained in the F3 range for 8 and 6 s, respectively, while remaining in or above the F2 range for 54 s (Fig. 16b). The mobile home was completely destroyed and removed from its foundation and thus met the f5 damage criteria. However, given that the structure was classified as a weak outbuilding, a −3 adjustment for structural integrity resulted in a final damage rating of F2.

A well-constructed frame house located about 60 m (one-half block) north of the mobile home was located just outside of the core-flow region, and the model gridpoint time series resembled that of the silo's gridpoint time series. The wind speed peaked at about 72 m s^{-1} for about 11 s and remained in or above the F2 category for 45 s. The house appeared to sustain only minor roof and siding damage, resulting in a final damage rating of only F1 with no structural integrity adjustment. Despite the fact that the mobile home and this frame house were both located approximately 30 m from the radius of maximum winds, and the model wind speed time series were very similar, there were large differences in

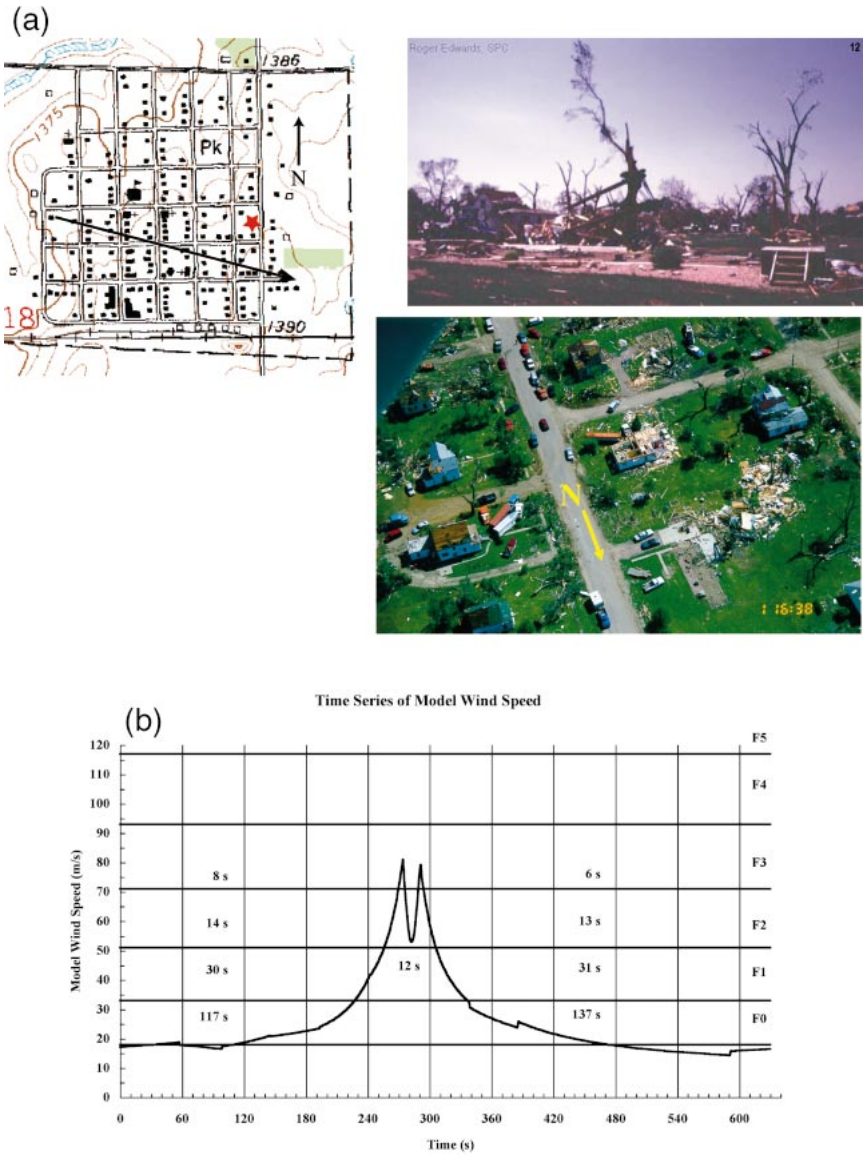

FIG. 16. F-scale comparison at a mobile home and well-constructed frame house located approximately 130 m north of the tornado track including (a) ground and aerial damage photography, which provided a damage F-scale estimate of F2 (courtesy of R. Edwards and B. Smith), and (b) a time series of the radar-constrained model wind speed (m s^{-1}) at the nearest grid point over this structure. The time duration of wind speeds in each F-scale category is shown for reference.

the observed damage between the structures. This example emphasizes the need to account for structural integrity to avoid a gross mischaracterization of the wind speed and resulting F-scale intensity. This example also suggests that relatively intense winds (72 m s^{-1}) can sometimes be associated with relatively light damage (F1) and challenges the hypothesis that damage can be defined as a unique function of peak wind speed and structural integrity. Other factors, including duration of intense winds, directional variability, and upstream debris loading may be important factors.

d. Model vertical profile

The radar-constrained model provided an estimate of the wind speed as a function of time at each grid point over the town of Spencer. However, these wind speeds were based upon Doppler velocity measurements centered around 30 m AGL, and not at building level (primarily 0 to 10 m AGL). The peak Doppler velocities in each scan of the volume observed between 0138:30 and 0139:15 UTC were used to calculate the peak tornado-relative and ground-relative wind speeds at every level. With single-Doppler data, the error in wind speed

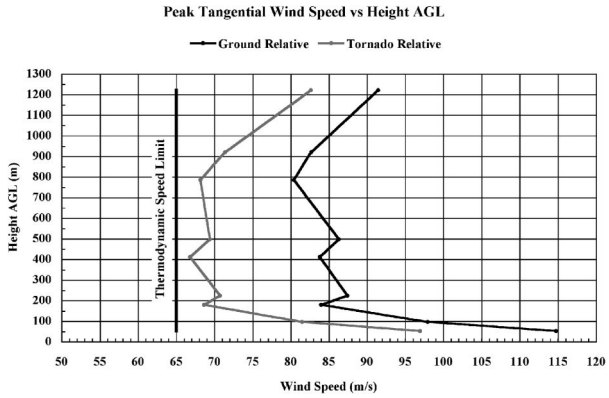

FIG. 17. Vertical profile of maximum tornado and ground-relative wind speeds from the radar-constrained model based upon the radar volume between 0138:30 and 0139:15 UTC as the tornado crossed the town of Spencer. Errors in the estimated peak horizontal wind speeds increase with height because of an increasing radar-beam crossing angle with the horizontal wind.

estimation increased at higher-elevation scans where larger components of the horizontal wind were not measured (Fig. 17).

Both the observed tornado and ground-relative wind speeds attained a maximum value in the lowest elevation scan (0.5°) at 30 m AGL, with values of 97 and 111 m s^{-1}, respectively. In the 200 m above this level these values decreased by about 60% to 69 and 84 m s^{-1} (Part I). This observation agrees with results from recent modeling studies of tornado vortex structure (Lewellen et al. 1997). From 200 to nearly 1000 m AGL, the wind speeds appeared to remain nearly constant at around 70 m s^{-1} for the peak rotational component, and about 85 m s^{-1} for the peak ground relative wind speed. Based upon the nearest sounding from Omaha, Nebraska, the estimate for CAPE in the local region around Spencer was at least 4000 J kg^{-1}. For a Rankine vortex, the theoretical thermodynamic speed limit in the region of this tornado is based upon the assumption that the radial pressure gradient is the result of a radial temperature gradient across a buoyant column of air (Fiedler and Rotunno 1986; Fiedler 1998) with the relation

$$V_{\max} = (\text{CAPE})^{1/2}. \quad (4.1)$$

This relation predicted a thermodynamic tornado-relative speed limit of about 65 m s^{-1} for the Spencer tornado. This speed limit is very similar to the radar observations of the peak rotational wind speeds in the region over 200 m AGL. The enhanced wind speeds in lowest 30 to 200 m appear to result from surface interaction (Lewellen et al. 1997).

Ideally, an estimate of the reduction in wind speeds from 30 to 3 m AGL was desired to represent the airflow at building level. However, there was insufficient information to attempt such an extrapolation in the turbulent surface layer of a violent tornado wind field, and there is both modeling and observational evidence that strong inflow occurs in the lowest several tens of meters (Lewellen et al. 2000; Wurman and Gill 2000; Part I). During the tornado's closest approach to the DOW, about 4 min before the tornado passed through Spencer, observations below 20 m AGL indicated peak winds that were about 16% lower than peak winds observed between 30 to 50 m AGL (Part I).

5. Sources of error

While both the damage survey information and Doppler radar velocities helped form an estimate of the Spencer tornado's intensity on the spatial scale of individual structures, there were complicating factors from both data sources. The radar-constrained model was limited to an axisymmetric structure that is only an idealization of the tornado vortex. To a first approximation the wind field across the tornado did appear to closely match that of the ideal vortex used in the model; there were clearly some perturbations to the flow that were not included in the model. The official damage survey concluded that the Spencer tornado was likely a single-vortex tornado as it passed through the town (USDOC 1998). The DOW3 radar observations occasionally showed hints of multiple-vortex structure (Part I). There are modulations in the damage pattern in Spencer that suggest the existence of weak multiple vortices with wind field perturbations significantly less than the basic wind field in the tornado. Northward protrusions of intense damage, greater than or equal to F3, existed west of Cordo Street, east of Fuller Street, and along and west of East Street (Fig. 4). These modulations in the damage pattern are spaced at intervals of approximately 300 m along the track of the tornado corresponding to 20-s differences in their time of occurrence. A single intense multiple-vortex-like, wavenumber-1 perturbation, rotating about the tornado at the radius of the peak rotational winds (175 m from the center) at about half of the peak rotational speed (48 m s^{-1}), would circle the tornado every 24 s, which is remarkably close to the temporal spacing of the more intense damage swaths.

Doppler velocity measurements were likely biased by large debris motion in the town and not necessarily representative of the air motion in the tornado's wind field (Dowell et al. 2001; DAWW). Furthermore, the beamwidth of the DOW radar over Spencer resulted in some averaging of the wind field, especially near the radius of maximum winds. However, given the relatively close proximity of the tornado to the radar, and the large size of the tornado, the aspect ratio was not low enough to prevent sampling of the core-flow region. With a typical sampling interval of about 35 m and an average tornado core-flow radius of about 150 m during this dataset, a Doppler velocity measurement of 100 m s^{-1} would have an aspect ratio adjustment of 6 m s^{-1}. When the tornado was passing through Spencer, this core-flow radius was actually closer to 200 m, thus reducing this sampling error to about 4 m s^{-1} (Wood and Brown 1997). The

Doppler velocity measurements represent the average motion of scatterers in a sample volume. In the highly turbulent region of the Spencer tornado, spectral width values often ranged between 12 and 15 m s^{-1}.

Two other biases contained in Doppler velocity measurements resulted from the influence of beam blockage and ground clutter. In the lowest tilts of each volume scan, at several kilometers range, the 3-dB beam and sidelobes intersected the ground and effectively dampened the resulting velocity measurement. While this effect was likely to be small given the flat terrain and slightly depressed deployment site, it cannot be totally ignored. Quality control steps were taken to discard Doppler velocities in regions where ground clutter from buildings or roads significantly contaminated the field.

The damage survey was also not without its limitations. The available photographs and damage survey documentation did provide information on many of the structure types in the town, but it was not possible to assess the building integrity of some structures that were severely damaged or destroyed. Another factor complicating the damage survey was the inability to account for opened garage doors either prior to or during the passage of the tornado, where the direction of the strong winds relative to the garage door opening would control a common starting point for progressive structural failure (Marshall 2002). There were also a few blocks in the town that lacked any significant structures, such as a park in the north-central portion. This lack of damage indicators resulted in interpolation of some F_D data. It was confirmed that significant damage cleanup had begun at first light on the morning after the tornado, which was several hours to even a day before most of the photographs were taken. Therefore, there was some contamination from the cleanup efforts in the damage photography. Finally, only distant aerial photographs were available for the northern portion of the town where little damage was observed. This distance made the detection of F0- and F1-type damage very difficult.

6. Conclusions

The Spencer tornado afforded the first opportunity to perform detailed comparisons between a damage survey and Doppler velocity measurements, given a radar-data-based evaluation of the Fujita scale. This evaluation established several facts about this tornado event that may be applicable to future studies:

(a) The F_R estimates at ~30 m AGL were generally higher than the F_D estimates in regions with and without significant structures. Part of this difference appeared to result from a wider rotational velocity field than necessary to produce the regions of observed damage. It was suspected that the broadening of the Doppler velocity core-flow signature might have resulted from debris centrifuging or tornado tapering.

(b) In this case, a primarily single-vortex tornado with a core-flow region approximately 350 m wide translated east-southeast with a forward motion of about 15 m s^{-1}. This translation was sufficient to induce an asymmetry in the strength of the wind field, thereby creating a difference of 1.0 to 1.5 F-scales on opposing sides of the tornado relative to its forward motion. The result was 30 m s^{-1} higher winds on the right side of the tornado's path and damage that was more widespread. Based on F_D, it appeared that most structures in the town remained intact at or below F2 wind speeds, but completely failed at or above F3 wind speeds largely due to inadequate construction. The F_R estimate indicated that the additional wind speed from translation on the right side of the track placed most of the structures in the southern three blocks of the town in the F3 or F4 range, while keeping most blocks north of the track in or below the F2 range. The result was that the highest and longest duration of winds were displaced southward from the center of the vortex track, and the center of the damage path was south of the center of the actual track of the tornado vortex.

(c) There were many severely damaged structures in Spencer located both within and outside the path of the core-flow region of the tornado. Model results from the radar data indicated two distinct evolutions in the wind field depending upon the region in which a structure resided. Structures inside the radius of maximum winds, such as the water tower, experienced both the core-flow and exponential-decay regions. This location resulted in a model wind time series with relatively large accelerations of the flow around 10 m s^{-2} in the core and a relatively short period of peak wind speeds. Structures outside the radius of maximum winds only experienced the exponential-decay region, but some endured a longer period of peak winds. We hypothesize that there are two modes of induced damage depending on the location of a structure relative to the tornado's location. A structure well within the core flow will experience two distinct periods of damaging winds from widely differing directions, while a structure outside the core might suffer only one, but perhaps a longer, period of damaging winds from a single preferred direction. The intensity of damage may be influenced by these differing wind duration and wind direction histories as well as by the peak wind gust, which is the sole meteorological factor accounted for in the Fujita scale.

(d) The radar-constrained model permitted the calculation of wind intensity metrics that incorporated intense wind speed duration, and other factors. The duration of intense winds and simple measures of the integrated effect of large debris impacts from these winds are well correlated with observed damage. While it was unclear whether these were better

correlated to observed damage than the traditional Fujita peak-wind-speed metric, the agreement was comparable. Since there are plausible physical mechanisms supporting these new metrics, these factors should be considered in future studies of damage intensity. Higher-resolution temporal measurements available with the rapid-scan DOW (Wurman and Randall 2001) may provide a means to differentiate among these various metrics.

(e) The variations of tornado wind speed as a function of height are most pronounced in the lowest 200 m AGL with the most extreme speeds observed below 50 m AGL. Current radar observations are unable to determine the exact elevation and magnitude of the true peak in tornado wind speeds, which appear to occur between the surface and 50 m AGL, or true winds at building level (0–10 m AGL). Given the practical limitations of both in situ and remotely sensed tornado wind speed observations near the surface where most structures and people reside, it is fundamentally important to continue to improve the characterization of the tornado flow through both observational and modeling efforts.

(f) Data obtained by the DOW for this study had unprecedented spatial and temporal resolution; however, the 50-s repeat intervals of near-ground observations were too infrequent to permit the tracking of sub-tornado-scale features or multiple vortices across Spencer in order to compare with smaller-scale damage features. More rapid updates every 5–10 s promised by the new rapid-scan DOW will be valuable in future studies.

Acknowledgments. This work was supported in part by National Science Foundation (NSF) Grant ATM-9703032. The DOWs are operated by the Center for Severe Weather Research (CSWR) and have been developed by the University of Oklahoma (OU), NCAR's Atmospheric Technology Division (ATD) (which is supported by the NSF), and the National Severe Storms Laboratory. Support for the DOW program has been received from the state of Oklahoma, the NSF, the CSWR, and the Office of Naval Research (ONR). David Dowell, Herbert Stein, and one of us (Wurman) crewed the DOW3 and were crucial in obtaining this dataset, collected in difficult circumstances. Mitch Randall, Jon Lutz, Jack Fox, and others at NCAR/ATD provided engineering support to develop the DOWs and to keep them running. Extensive damage survey photography, notes, and personal communication were provided by Brain Smith of the National Weather Service (NWS), Long Phong of the National Institute for Standards and Technology's (NIST) structures division, and Roger Edwards from the Storm Prediction Center (SPC). Roger Edwards and Greg Harmon from the NWS also provided data from the F-scale exercise at the 1998 NWS/Texas Tech Severe Storms Conference in Lubbock, Texas. Pengfei Zhang of the National Severe Storms Laboratory assisted with processing of the data. Alan Shapiro and John Snow of OU provided scientific input and suggestions. This work was also assisted by an American Meteorological Society/NWS graduate student fellowship.

REFERENCES

Alexander, C. R., and J. Wurman, 2005: The 30 May 1998 Spencer, South Dakota, storm. Part I: The evolution and environment of the tornadoes. *Mon. Wea. Rev.*, **133,** 72–96

Bluestein, H. B., and A. L. Pazmany, 2000: Observations of tornadoes and other convective phenomena with a mobile, 3-mm wavelength, Doppler radar: The spring 1999 field experiment. *Bull. Amer. Meteor. Soc.*, **81,** 2939–2951.

——, ——, J. C. Galloway, and R. E. McIntosh, 1995: Studies of the substructure of severe convective storms using a mobile 3-mm-wavelength Doppler radar. *Bull. Amer. Meteor. Soc.*, **76,** 2155–2169.

Doswell, C. A., III, and D. Burgess, 1988: On some issues of United States tornado climatology. *Mon. Wea. Rev.*, **116,** 495–501.

Dowell, D. C., J. Wurman, and L. Wicker, 2001: Centrifuging of scatterers in tornadoes. Preprints, *30th Conf. on Radar Meteorology*, Munich, Germany, Amer. Meteor. Soc., 307–309.

——, C. Alexander, J. Wurman, and L. Wicker, 2005: Centrifuging of hydrometeors and debris in tornadoes: Radar-reflectivity patterns and wind-measurement errors. *Mon. Wea. Rev.*, in press.

Edwards, R., 2003: Rating tornado damage: An exercise in subjectivity. Preprints, *First Symp. on F-Scale and Severe-Weather Damage Assessment*, Long Beach, CA, Amer. Meteor. Soc., 503–504.

Fiedler, B. H., 1998: Wind-speed limits in numerically simulated tornadoes with suction vortices. *Quart. J. Roy. Meteor. Soc.*, **124,** 2377–2392.

——, and R. Rotunno, 1986: A theory for the maximum windspeeds in tornado-like vortices. *J. Atmos. Sci.*, **43,** 2328–2340.

Fujita, T. T., 1971: Proposed characterization of tornadoes and hurricanes by area and intensity. SMRP Res. Rep. 91, University of Chicago, 15 pp.

——, 1973: Experimental classification of tornadoes in FPP scale. SMRP Res. Rep. 98, University of Chicago, 15 pp.

——, 1992: *Mystery of Severe Storms.* The University of Chicago Press, 298 pp.

——, and B. E. Smith, 1993: Aerial survey and photography of tornado and microburst damage. *The Tornado: Its Structure, Prediction, and Hazards*, *Geophys. Monogr.*, No. 79, Amer. Geophys. Union, 479–493.

Letzmann, J., 1923: Das Bewegungsfeld im Fuss einer fortschreitenden Wind-oder Wasserhose (The flow field at the base of a progressing tornado). Ph.D. dissertation, Tartu Ülikool, 136 pp. [Available online in German at http://www.essl.org/pdf/Letzmann1923/Letzmann1923.pdf.]

Lewellen, D. C., W. S. Lewellen, and J. Xia, 2000: The influence of a local swirl ratio on tornado intensification near the surface. *J. Atmos. Sci.*, **57,** 527–544.

Lewellen, W. S., D. C. Lewellen, and R. I. Sykes, 1997: Large-eddy simulation of a tornado's interaction with the surface. *J. Atmos. Sci.*, **54,** 581–605.

Marshall, T. P., 1983: Utilization of load and resistance statistics in a wind speed assessment. M.S. thesis, Dept. of Civil Engineering, Texas Tech University, 91 pp.

——, 1992: Lessons learned from analyzing tornado damage. *The Tornado: Its Structure, Dynamics, Prediction, and Hazards*, *Geophys. Monogr.*, No. 79, Amer. Geophys. Union, 495–499.

——, 2002: Tornado damage survey at Moore, Oklahoma. *Wea. Forecasting*, **17,** 582–598.

——, 2004: The enhanced Fujita (EF) scale. Preprints, *22d Conf. on*

Severe Local Storms, Hyannis, MA, Amer. Meteor. Soc., CD-ROM, 3B.2.

McDonald, J. R., 2001: T. Theodore Fujita: His contribution to tornado knowledge through damage documentation and the Fujita scale. *Bull. Amer. Meteor. Soc.*, **82,** 63–72.

——, and T. P. Marshall, 1984: Tornado damage documentation. Institute for Disaster Research Publication 1984-20, Texas Tech University, 27 pp.

Mehta, K. C., 1976: Windspeed estimates: Engineering analysis. *Proc. Symp. on Tornadoes*, Lubbock, TX, Texas Tech University, 89–103.

Peterson, R. E., 1992a: Johannes Letzmann: A pioneer in the study of tornadoes. *Wea. Forecasting*, **7,** 166–184.

——, 1992b: Letzmann's and Koschmieder's ''Guidelines for research on funnels, tornadoes, waterspouts and whirlwinds.'' *Bull. Amer. Meteor. Soc.*, **73,** 597–611.

Snow, J. T., 1984: On the formation of particle sheaths in columnar vortices. *J. Atmos. Sci.*, **41,** 2477–2491.

USDOC, 1998: Service assessment: Spencer, South Dakota, tornado May 30, 1998. NOAA/NWS, 18 pp.

Wood, V. T., and R. A. Brown, 1997: Effects of radar sampling on single-Doppler velocity signatures of mesocyclones and tornadoes. *Wea. Forecasting*, **12,** 928–938.

Wurman, J., 1999: Preliminary results from the Radar Observations of Tornadoes and Thunderstorm Experiment (ROTATE-98/99). Preprints, *29th Conf. on Radar Meteorology*, Montreal, QC, Canada, Amer. Meteor. Soc., 613–616.

——, 2001: The DOW mobile multiple-Doppler network. Preprints, *30th Conf. on Radar Meteorology*, Munich, Germany, Amer. Meteor. Soc., 95–97.

——, 2002: The multiple-vortex structure of a tornado. *Wea. Forecasting*, **17,** 473–505.

——, and S. Gill, 2000: Finescale radar observations of the Dimmitt, Texas (2 June 1995), tornado. *Mon. Wea. Rev.*, **128,** 2135–2164.

——, and M. Randall, 2001: An inexpensive, mobile, rapid-scan radar. Preprints, *30th Conf. on Radar Meteorology*, Munich, Germany, Amer. Meteor. Soc., 98–100.

——, J. M. Straka, and E. N. Rasmussen, 1996a: Fine-scale Doppler radar observations of tornadoes. *Science*, **272,** 1774–1777.

——, ——, and ——, 1996b: Preliminary radar observations of the structure of tornadoes. Preprints, *18th Conf. on Severe Storms*, San Francisco, CA, Amer. Meteor. Soc., 17–22.

——, M. Randall, and A. Zahrai, 1997: Design and deployment of a portable, pencil-beam, pulsed, 3-cm Doppler radar. *J. Atmos. Oceanic Technol.*, **14,** 1502–1512.

Zrnić, D., D. W. Burgess, and L. Hennington, 1985: Doppler spectra and estimated windspeed of a violent tornado. *J. Appl. Meteor.*, **24,** 1068–1081.